ISSN 2007-9737

Design and Implementation of an Automatic Control System using Motors and Control Sensors to Stabilize a Horizontal Platform with a LiDAR Sensor

José Antonio Taquía Gutiérrez, Paul Quiroz Villalobos

Universidad de Lima,
Instituto de Investigación Científica,
Peru

{jtaquia, pquiroz}@ulima.edu.pe

Abstract. Laser imaging detection and ranging (LiDAR) sensors can be used in numerous applications mainly due to their ability to measure distances or perform 3D surface mappings. However, to perform these functions efficiently in certain situations, such as in a moving vehicle, LiDAR sensors require a stabilizing platform to prevent terrain irregularities from affecting their measurements. Moreover, accurate platform control is one of the main challenges of modern control engineering. Although several approaches concerning this challenge have been proposed, the high computational cost of control algorithms continues to be their largest drawback. Within this context, the present work seeks to implement a control system to achieve the horizontal stabilization of a two-degree-of-freedom platform for a LiDAR sensor using inertial systems and embedded software platforms, thereby guaranteeing not only portability but also low computational costs.

Keywords. Sensors, Arduino, Matlab, Simulink, PID, Gimbal, LiDAR.

1 Introduction

Most platform stabilization devices are currently used in various fields for different purposes. For example, LiDAR devices use laser-based remote sensing technology [6]. In this sense, because LiDAR is advantageous in capturing the environment, it is used in geographic information systems (GIS) to generate digital terrain models (DTM) for 3D mappings [1,13]. Unlike other technologies, such as traditional photometry or overlay analysis image processing, a radar seeker might be an efficient option for developing robust moving application alternatives.

Furthermore, as different types of motors, such as servomotors or brushless DC motors, can be used for platform stabilization, responses from sensors are likely to be different from one another [9, 11]. Proportional, integrative and derivative (PID) control is an approach to obtain accurate responds to changes on systems. There are different types of tunning rules depending on gains of their elements [7]. Moreover, other studies have proposed using control systems to set a target point using regions of interest on images and apply a PID logic to control a gimbal [9]. Herein, analysis tools such as Simulink and Matlab are used to describe the operation of DC motors considering the parameters that influence their speed control [2]. Moreover, the dynamics of a dc motor are part of the definition of the system type and the plant parameter to be model on Simulink [3]. In this work, we describe a platform movement changes considering the influence stabilization parameters as well as the impact from applying optimized control strategies using prototypes on the Simulink tool.

2 Development Methodology

The proposed design is aimed at providing stability to a horizontal LiDAR sensor platform. To achieve this objective, we used an iterative and incremental development model with well-differentiated phases or milestones for each development process stage. The phases considered and their corresponding scopes are described below.

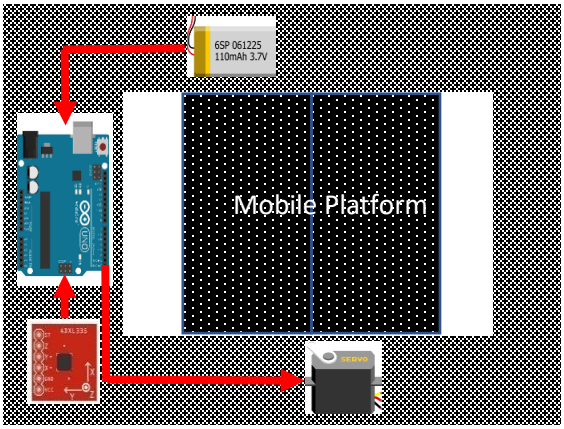

Fig. 1. One-dimensional prototype

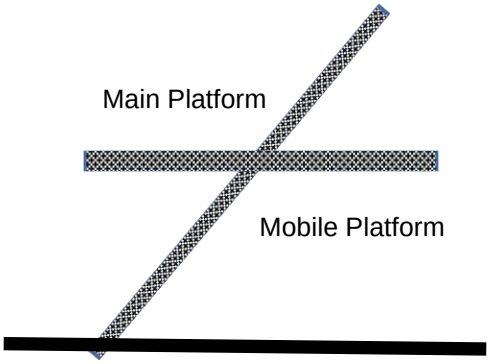

Fig. 2. Platform design

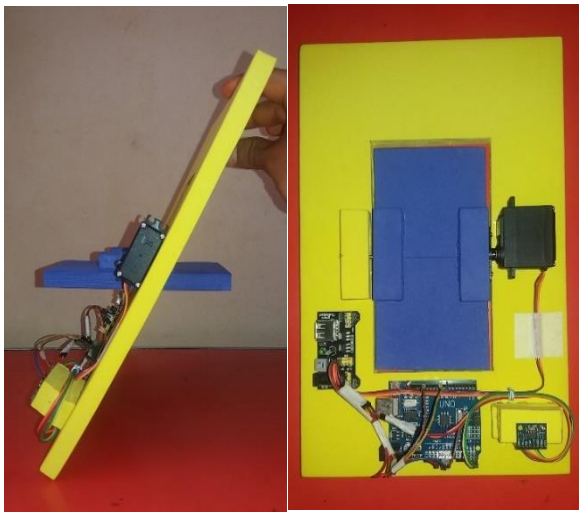

Fig. 3. Working platform

a) Phase I: One-dimensional (1D) stability control
b) Phase II: Two-dimensional (2D) stability control
c) Phase III: Moving platform distance measurements using the LiDAR sensor.

3 Design Description

3.1 Phase I: One-Dimensional (1D) Control

To achieve a state of equilibrium with a degree of freedom, when the main platform shifts between 0 and 180 degrees, the mobile platform must gradually modify its position to always remain parallel to the horizontal reference base. The schematic designs for Phase I as well as the devices used and their operation principles are described below:

Figure 1 provides a top view of the diagrams developed for Phase I of the Project.

Figure 2 provides a side view of Fig. 1, wherein the angle formed between the main and mobile platforms can be observed.

Figure 3 denotes the actual Phase I implementation.

3.2 Phase II: Two-Dimensional (2D) Control

The Inventor tool was used to design the 2D prototype. This tool is a parameter-driven 3D solid modeling suite supported by the AutoDesk Company. The prototype components designed were then printed on a 3D printer. The prototype includes mobile joints that provide three degrees of freedom, one for each x, y, and z axis, denominated as roll, pitch, and yaw respectively, as well as a support for the LiDAR sensor [8].

To achieve a state of equilibrium with two degrees of freedom, when the main platform of the prototype (shown in purple) shifts between 0 and 180 degrees along the x or y axes, the mobile platform that supports the LiDAR sensor must gradually modify its position to always remain parallel to the horizontal reference base.

Figure 5 denotes the actual implementation of the 2D prototype, wherein the TF Mini Plus LiDAR sensor may be observed already installed in the support.

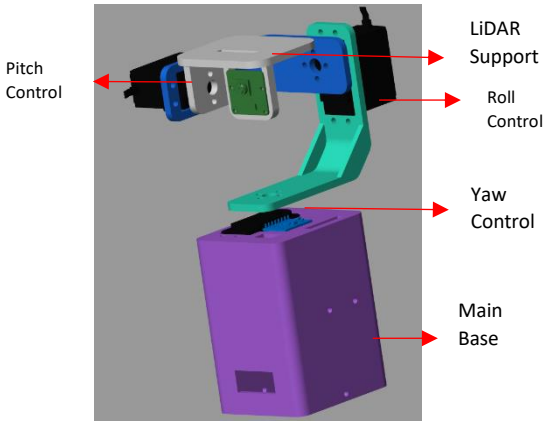

Fig. 4. CAD structure

Fig. 5. Structure with LiDAR

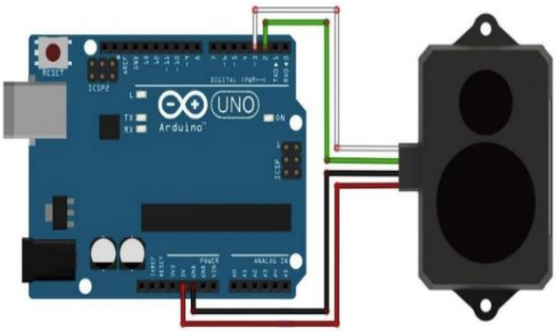

Fig. 6. Arduino connections with LiDAR

3.3 Phase III: Moving Platform Distance Measurements Using the LiDAR Sensor

We used the TF Mini Plus sensor to measure distances. This is a time of flight (ToF) sensor capable of measuring objects located at 10 cm to 12 m. It is powered with 5 V and can send information through the serial port at 115,200 bauds.

Figure 6 denotes the connection between the TF Mini Plus sensor and Arduino UNO module.

The following table lists the specifications for the TF Mini Plus sensor used.

3.4 Components Used

3.4.1 Accelerometer

According to Newton's second law:

$$\vec{F} = m \cdot \vec{a}.$$

From the above expression, a body with a mass of "m" subjected to acceleration will experience a force "F" that is proportional to the said acceleration. This force is used to activate the internal micro-mechanized structure of the accelerometer, through which the acceleration of the body may be measured independently in each of the three X, Y, and Z axes.

Moreover, when the acceleration values from each axis are combined, the angle of inclination at which the body is with respect to each plane can be trigonometrically calculated, as shown in Fig. 7. For the purposes hereof, the ADXL345 accelerometer has been used to determine the pitch and roll inclination angles of the main base. Figure 8 displays the connection diagram between the ADXL345 module and Arduino UNO platform.

3.4.2 Servomotor

A servomotor (or servo) is a special type of direct current (DC) motor that provides controlled rotation movements and high torque. For these two features, servomotors require a pulse-width-modulation (PWM)-based control signal and gearbox.

Figure 9 illustrates the block diagram for a servomotor control system.

To implement the 2D platform, we used two Tower Pro MG995 servomotors. Each motor provides a torque of 15 Kg-cm and the maximum

Table 1. Sensor specifications

Range	0.1–12 m
Accuracy	+5 cm (0.1–6 m); 1% (6–12 m)
Resolution	5 mm
Frequency	1–1000 Hz
Sensibility	70 k lux
Temperature	−20°C–60°C

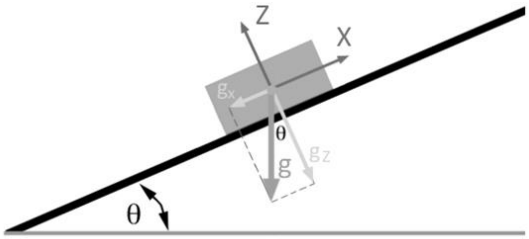

$$\theta = atan\frac{A_x}{A_z}$$

Fig. 7. Angle of inclination

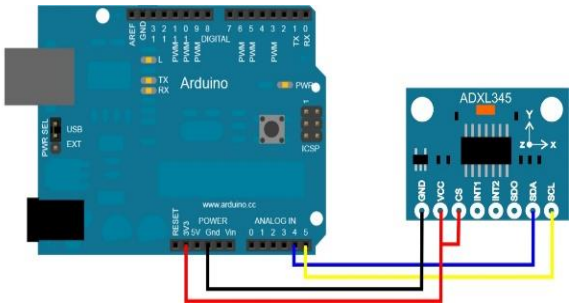

Fig. 8. Arduino–accelerometer connection

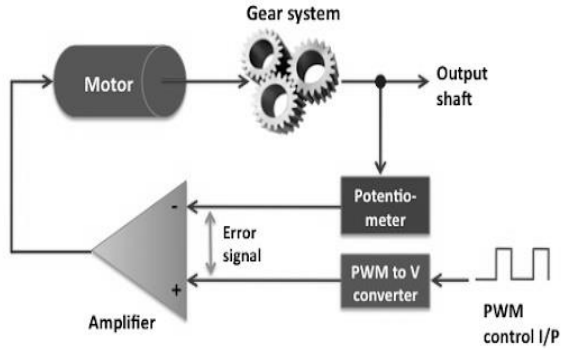

Fig. 9. Block chart

rotation angle of 180 degrees at an operating voltage of 4.8–7.2 V.

3.5 Mathematical Motor Model

The servomotor system uses the DC motor to control the mechanical position of the rotor according to the voltage supplied by a magnetic field [5]. Figure 10 illustrates the motor used in the present work [10].

Using Kirchhoff's law of voltage, the following equation is obtained:

$$V_a(t) = R_a\, i_a(t) + L_a \frac{di(t)}{dt} + Eb(t).$$

The torque (*T*) of the motor for the armature load "*i*" with a (K) factor:

$$T = Ki.$$

The Counter EMF (Eb) related to the angular velocity:

$$Eb = K\omega = k\frac{d\theta}{dt}.$$

Regarding the model of a DC motor and Newton's law combined with Kirchhoff's law:

$$J\frac{d2\theta}{dt} + b\frac{d\theta}{dt} = Ki, \tag{1}$$

$$L\frac{di(t)}{dt} + Ri = V - K\frac{d\theta}{dt}. \tag{2}$$

Using Laplace, Equations (1) and (2) can be restated as:

$$JS^2\theta(s) + bS\theta(s) = KI(s), \tag{3}$$

$$LSI(s) + RI(s) = V(s) - KS\theta(s). \tag{4}$$

Then, from Equations (3) and (4), we obtain Equation (5):

$$I(s) = \frac{V(s)-KS\theta(s)}{R+LS},$$
$$JS^2\theta(s) + bS\theta(s) = K\frac{V(s) - KS\theta(s)}{R + LS}. \tag{5}$$

The block diagram for the DC motor is displayed in Fig. 11.

In Equation (6), we obtain the transfer function with an output angle of θ as a function of voltage (V(s)):

$$G_a(s) = \frac{\theta(s)}{V(s)} = \frac{K}{S[(R + LS)(JS + b) + K2]}. \tag{6}$$

Considering the DC motor diagram from Fig. 11, Equation (7) provides the transfer function for the angular velocity (ω) against the input (V(s)).

$$G_v(s) = \frac{\omega(s)}{V(s)} = \frac{K}{[(R + LS)(JS + b) + K2]}. \quad (7)$$

From Equation (7), we can obtain the transfer function Equation (8):

$$\frac{\omega(s)}{V(s)} = \frac{K}{(LJ)S2 + (RJ + Lb)S + (Rb + K2)}. \quad (8)$$

Here:

V_a = the armature wherein the coil is contained (V) (Input),

R_a = armature resistance (Ω),

L_a = armature inductance (H),

i_a = current passing through the armature (A),

E_b = counter electromotive force (counter EMF) (V),

T = torque (Nm),

θ = rotor angular position (rad) (output).

3.6 Control Strategies

In this work, we used three control strategies, and each one is assessed below:

3.6.1 Pulse-Width-Modulation-Based Serial Proportional Controller

PWM is one of the most efficient servomotor control techniques. It generates a periodic square wave wherein the wave portion that remains in the high state of the signal will be proportional to the distance that the motor will travel.

The timer contains the pulse width in a micro-controller; therefore, when the overflow occurs, the PWM signal will remain high until the moment when the comparator generates an interruption after the pulse has elapsed. The length of the pulse will indicate the angle of the rotation of the motor.

Figure 12 contains some examples of typical angular positions for a servomotor and the corresponding control pulses.

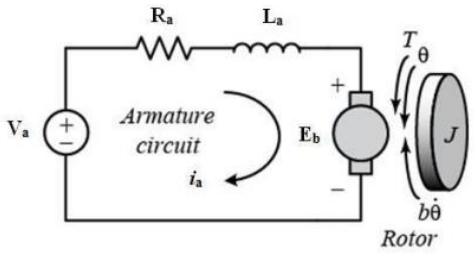

Fig. 10. DC motor

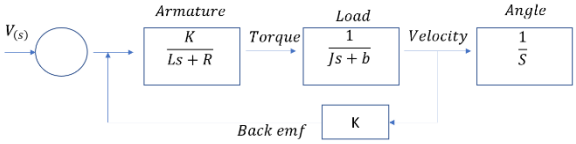

Fig. 11. Block diagram

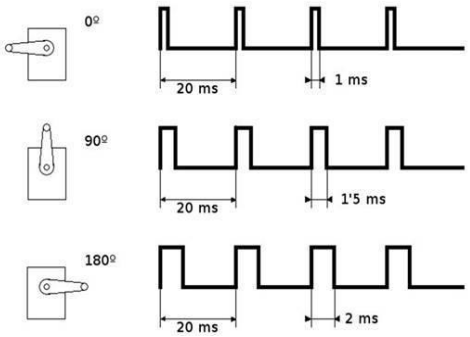

Fig. 12. PWM chart

For the servomotor to be positioned and held in the desired location, regardless of disturbances or external forces to which it may be subjected, the proportional control must be serially applied and sustained over time.

3.6.2 Proportional Integrator Derivative (PID) Controller

The PID controller was implemented in the design using the Simulink/Matlab PID Controller block. This block optimizes the parameters of the PID control function [5].

To improve the performance of the stabilization response, we used a PID controller in the 3D prototype designed. Thereafter, it was replicated in Simulink (a Matlab modeling software) and Sim

ISSN 2007-9737

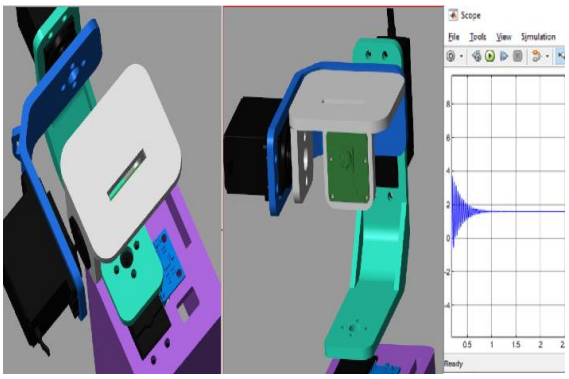

Fig. 13. Overshoot and vibration

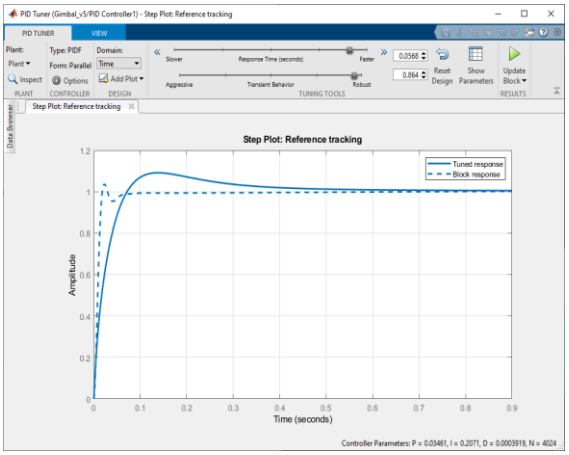

Fig. 14. Block respond and tuned respond with Matlab

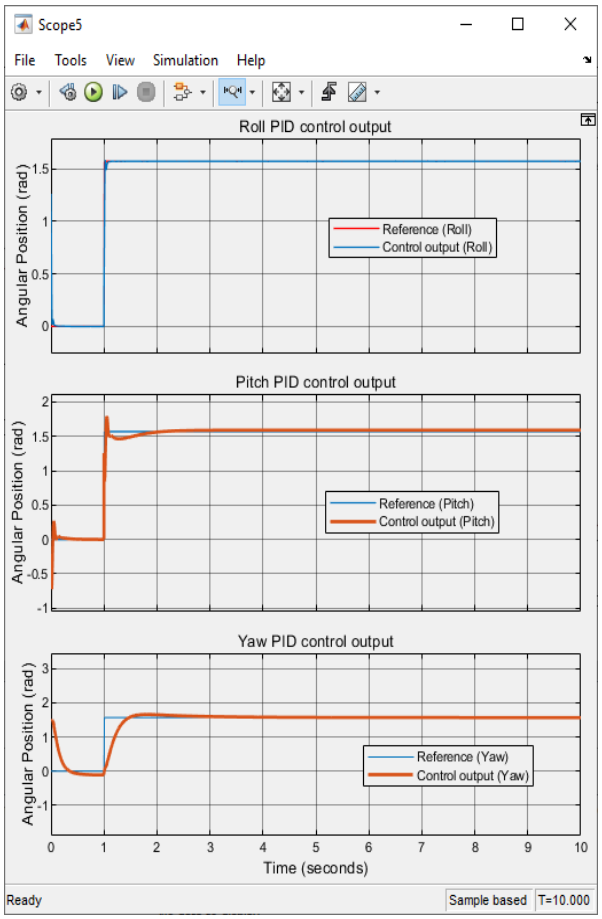

Fig. 15. PID-based stability

Mechanics, and the proportional, integral, and derivative control parameters were defined.

Figure 13 denotes the behavior of the Z axis before the optimization of the PID parameters. Therein, the overshoot and unwanted vibration of the platform can be observed.

Finally, Fig. 14 denotes the results from the stability analysis using the PID controls that were obtained from physical prototype tests.

Figure 15 denotes the results from the stability analysis after applying the PID controller to the physical prototype.

As can be observed, the pitch and yaw exhibit a slight short and overshoot, which is then offset, achieving the system stabilization. Moreover, the roll control evidences one with the best results, with an overshoot close to zero. Figure 16 shows the roll results for the fuzzy logic controller.

3.7 Tests and Results

The distance measurement tests toward a fixed target located 2.40 m off the LiDAR sensor, with the platform in motion, are denoted.

As the pitch angle decreases, the platform slightly approaches the target, and the distance detected by the sensor decreases. As the pitch angle increases, the platform slightly moves away from the target, and the distance detected by the sensor increases. In both the cases, the distance variation is minimal mainly because the LiDAR sensor is always kept in a horizontal position pointing toward the target.

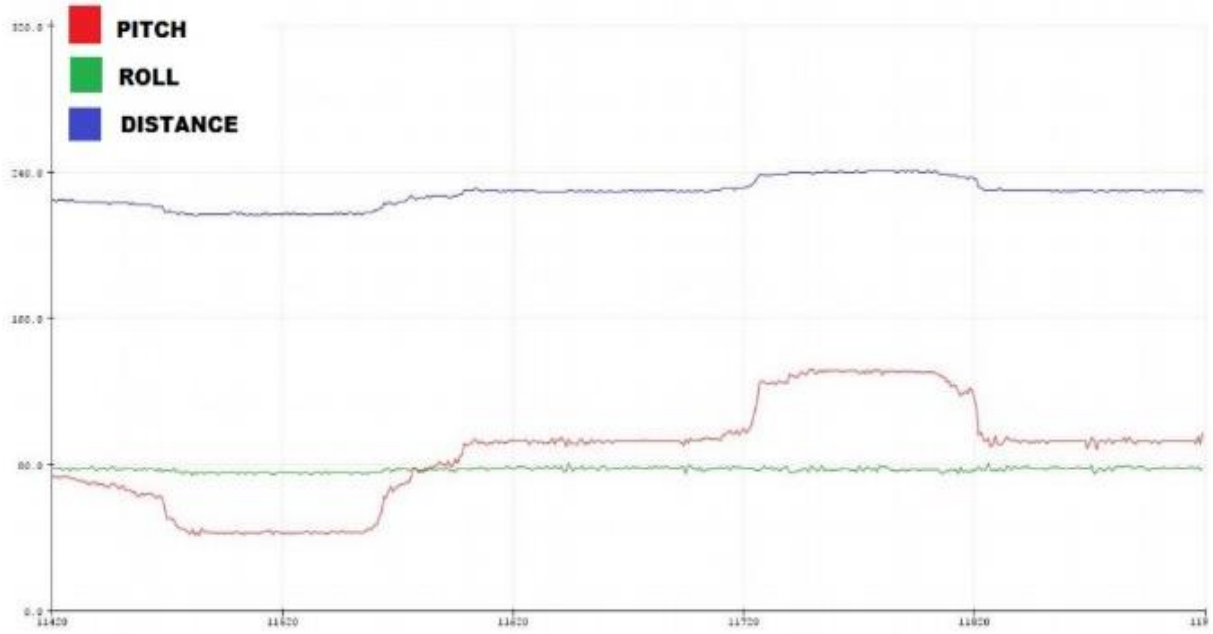

Fig. 16. 2D output signal

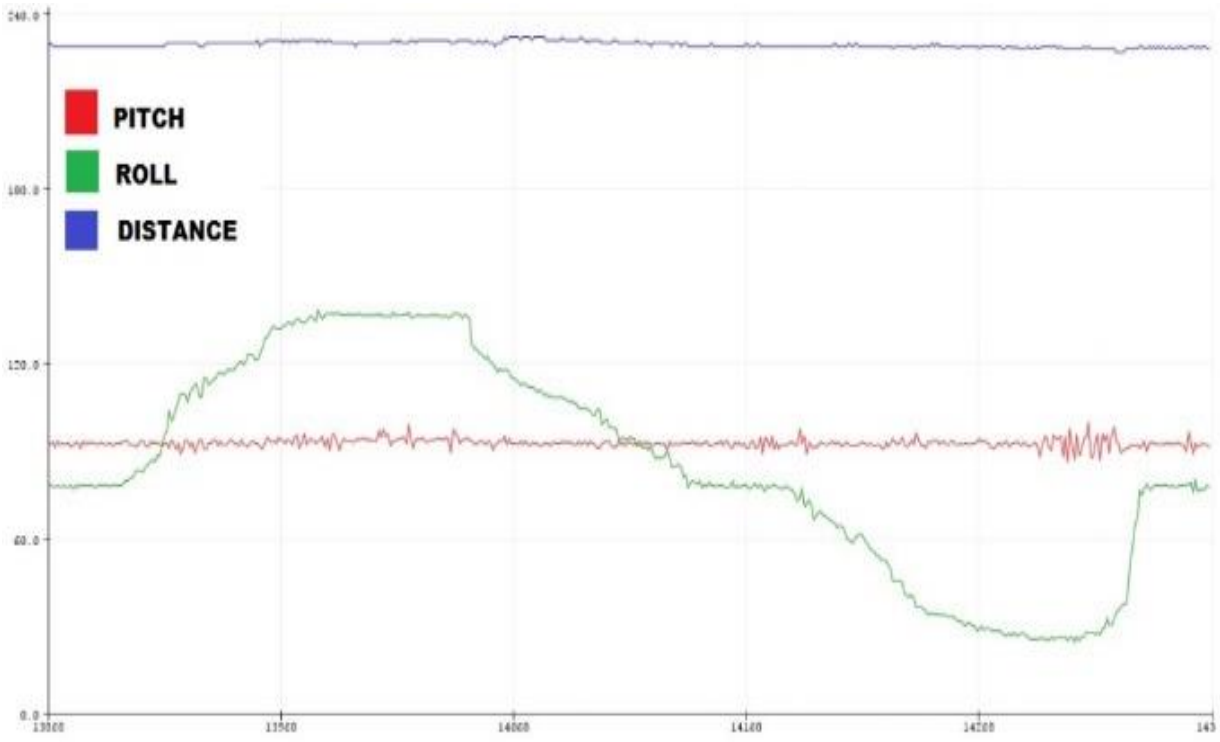

Fig. 17. 2D output signal

Figure 17 denotes the tests results when changing the roll angle.

At different roll angles, when changing the position of the platform toward the sides in parallel direction to the target, the distance detected by the LiDAR sensor remains constant.

These results are expected because the roll controller always maintains the sensor in the same horizontal position from the target.

4 Conclusions

The following conclusion are drawn:

- The stabilization control system of a horizontal platform has proven to be a very useful tool whenever the platform is in motion, and sensor position must be held constant against a target. This is very useful in applications such as sensors in photo cameras, moving terrestrial vehicles, or aquatic vehicles.
- Servomotors are a very efficient alternative for the other types of direct current motors that require an accurate control of their angular positions.
- In this light, the accelerometer is an essential device to determine the inclination or acceleration components of an object with respect to the ground.
- Moreover, the PWM-based proportional control strategy has been proven effective in controlling the angular position of a motor.
- Further, the PID control strategy is extremely robust. However, the biggest challenge lies in setting forth optimal values for the proportional, integral, and derivative gain parameters.

The data description and explanation are available at the links (1) Simulink and sim mechanics[1], (2) Control tests in two dimensions[2].

[1] https://drive.google.com/file/d/1YkM6DVN6uHoGtKiFXQNDHT6H13_OHX-8/view?usp=sharing

References

1. **Gašparović, M., Jurjević, L. (2017).** Gimbal influence on the stability of exterior orientation parameters of UAV acquired images. Sensors, Vol. 17, No. 2, pp. 401. DOI: 10.3390/s 17020401.
2. **Hammoodi, S.J., Flayyih, K.S., Hamad, A.R. (2020).** Design and implementation speed control system of DC Motor based on PID control and Matlab Simulink. International Journal of Power Electronics and Drive Systems, Vol. 11, No. 1, pp. 127–134. DOI: 10.11591/ijpeds.v11.i1.
3. **Hasan, S., Sarowar, G. (2020).** Simulation for improvement of DC motor controllers' response with application to a mobile robot. International Journal of Power Electronics and Drive Systems, Vol. 11, No. 2, pp. 580–593. DOI: 10.11591/ijpeds.v11.i2.
4. **Ketthong, T., Tunyasirut, S., Puangdownreong, D. (2017).** Design and implementation of I-PD controller for DC motor speed control system by adaptive tabu search. International Journal of Intelligent Systems and Applications, Vol. 9, No. 9, pp. 69. DOI: 10.5 815/ ijisa.2017.09.08
5. **Keviczky L., Bars R., Hetthéssy J., Bányász C. (2019).** Description of continuous systems in the time-, operator- and frequency domains. Control Engineering: MATLAB Exercises. Advanced Textbooks in Control and Signal Processing. Springer, Singapore. DOI: 10.10 07/978-981-10-8321-1_2.
6. **Lee, K.H. (2020).** Improvement in target range estimation and the range resolution using drone. Electronics, Vol. 9, No. 7, pp. 1136. DOI: 10.3390/electronics9071136.
7. **Mhawesh, M. A. (2021).** Performance comparison between variants PID controllers and unity feedback control system for the response of the angular position of the DC motor. International Journal of Electrical and Computer Engineering, Vol. 11, No. 1, pp. 802–814. DOI: 10.11591/ijece.v11i1.pp802-814.
8. **Naderolasli, A., Ataei, M. (2020).** Stabilization of A two-DOF gimbal system using direct self-tuning regulator. International Journal on Electrical Engineering and Informatics, Vol. 12, No. 1, pp. 33–44. DOI: 10.15676/ijeei.2020. 12.1.3.
9. **Park, H.C., Lee, S.W., Jeong, H. (2020).** Image-based gimbal control in a drone for centering photovoltaic modules in a thermal image. Applied Sciences, Vol. 10, No. 13, pp. 4646. DOI: 10.3390/app10134646.

[2] https://drive.google.com/file/d/1vkAcLnf1XCY8ZK6rtNdRtaJ94zyVPRkH/view?usp=sharing

10. **Rahman, Z.A.S. (2017)**. Design a fuzzy logic controller for controlling position of dc motor. Int. J. Comput. Eng. Res., Trends, Vol. 4, pp. 285–289.
11. **Shi, Z., Song, H., Chen, H., Sun, Y. (2018).** Research on measurement accuracy of laser tracking system based on spherical mirror with rotation errors of gimbal mount axes. Review Measurement Science, Vol. 18, No. 1, pp. 13–DOI: 10.1515/msr-2018-0003.
12. **Tomoiagă, T., Predoi, C., Coşereanu, L. (2016).** Indoor mapping using low-cost LIDAR based systems. Applied Mechanics and Materials, Vol. 841, pp. 198–205. DOI: 10.4028/www.scientific.net/AMM.841.198.

Article received on 06/03/2021; accepted on 15/08/2021.
Corresponding author is José Antonio Taquía Gutiérrez.